Theoretical Investigation of Oxygen-17 NMR Shielding and Electric Field Gradients in Glutamic Acid Polymorphs

Jonathan R. Yates,* Chris J. Pickard, and Mike C. Payne

Cavendish Laboratory, Cambridge, CB3 0HE, United Kingdom

Ray Dupree

Department of Physics, University of Warwick, Coventry, CV4 7AL, United Kingdom

Mickael Profeta and Francesco Mauri

Laboratoire de Minéralogie-Cristallographie de Paris, Université Pierre et Marie Curie, 4 Place Jussieu, 75252, Paris, Cedex 05, France

Received: February 12, 2004; In Final Form: May 6, 2004

We present an assignment of the experimental ^{17}O NMR shielding parameters for L-glutamic acid·HCl (Lemaitre, V.; Pike, K. J.; Watts, A.; Anupold, T.; Samoson, A.; Smith, M. E.; Dupree, R. *Chem. Phys. Lett.* **2003**, *371*, 91) based on first-principles quantum mechanical calculations. We use density functional theory and the gauge-including projector-augmented wave method (Pickard, C. J.; Mauri, F. *Phys. Rev. B* **2001**, *63*, 245101), which treats the true periodic nature of the crystal structure. We perform further theoretical calculations on a range of glutamic acid polymorphs and draw general conclusions about the influence of hydrogen bonding on ^{17}O NMR shielding parameters.

1. Introduction

Oxygen is an important element in organic and biological molecules since it is often intimately involved in hydrogen bonding. Solid-state ^{17}O NMR should be a uniquely valuable probe as the chemical shift range of ^{17}O covers almost 1000 ppm in organic molecules.[1,2] Furthermore ^{17}O has spin $I = {}^5/_2$ and hence a net quadrupole moment. As a consequence of this, the solid state NMR spectrum is strongly affected by the electric field gradient (EFG) at the nucleus, a quantity which is known to be extremely sensitive to molecular geometry. As the isotopic abundance of ^{17}O is very low (0.037%) and the NMR line widths due to the EFG relatively large, only limited solid-state NMR data is available.[3−5] However, in a recent paper, Lemaitre et al.[6] have reported ^{17}O magic-angle Spinning (MAS) NMR spectra for L- and D-glutamic acid·HCl. While it was possible to resolve peaks from each atomic site, it was not possible to provide an unambiguous assignment of the spectra.

First principles quantum mechanical calculations of shielding parameters have proven to be a useful tool in assigning experimental NMR spectra.[7,8] Traditional quantum chemistry codes are able to calculate NMR shielding parameters for isolated systems. To calculate shielding parameters for an extended system, such as a molecular crystal, it is necessary to construct a cluster of molecules such that the site of interest has the same local environment as in the full crystal.[4] Rather than use a cluster approach, we use a recently developed method[9] based on density functional theory (DFT) and the plane-wave pseudopotential approach,[10] which allows the calculation of shielding parameters in periodic systems. This implicitly accounts for intermolecular effects by using the translational symmetry present in a crystal. The method has previously been applied to the calculation of ^{17}O shielding parameters in zeolites[11] giving excellent agreement with experiment and improving significantly on earlier cluster calculations.[12]

In this paper, we apply the method of ref 9 to calculate the ^{17}O shielding parameters in L-glutamic acid·HCl and assign the experimental spectra. We further calculate shielding parameters for three polymorphs of glutamic acid whose experimental spectra are unknown. These studies allow correlations to be found between ^{17}O NMR shielding parameters and hydrogen bonding in the crystal structure.

2. Definitions and Methods

The crystal structures for anhydrous α-L-glutamic acid (α-L-Glu),[13] anhydrous β-L-glutamic acid (β-L-Glu),[14] anhydrous DL-glutamic acid (DL-Glu),[15] and L-glutamic acid·HCl (L-Glu·HCl)[16] were taken from the Cambridge Structural Database.[17] The structure of DL-Glu had been determined by X-ray diffraction and the other three structures by neutron diffraction. Positions of hydrogen atoms determined by X-ray diffraction are known to be less accurate than those given by neutron diffraction; in particular, hydroxyl bonds are significantly shorter than those given by neutron diffraction.[18] For consistency, partial geometry optimizations were performed for each structure, starting with the experimental structure and allowing the positions of the hydrogen atoms to relax. To perform the geometry optimizations, we use the DFT code CASTEP.[19] This uses a plane-wave basis set to expand the charge density and electronic wave functions. Pseudopotentials are used to represent the core electrons. We use the PBE[20] exchange-correlation functional and ultrasoft pseudopotentials[21] with a maximum plane-wave cutoff energy of 30 Ryd.

Chemical Shielding. The chemical shieldings were computed using the PARATEC[22] code following the method of ref 9. The calculations used Trouiller−Martins[23] norm-conserving pseudopotentials and the PBE[20] exchange-correlation functional. The

* To whom correspondence may be addressed. E-mail: jry20@cam.ac.uk.

10.1021/jp049362+ CCC: $27.50
Published on Web 06/17/2004

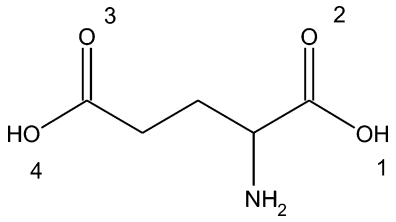

Figure 1. Chemical structure of glutamic acid with oxygen sites labeled.

wave functions are expanded in plane waves with a maximum energy of 80 Ryd, which previous studies have shown to give fully converged shielding parameters.[11]

The output of a first-principles NMR calculation is the absolute chemical shielding tensor, $\bar{\sigma}$, defined as the ratio between a uniform external magnetic field, **B**, and the induced magnetic field, $\mathbf{B}_{in}(\mathbf{r})$

$$\mathbf{B}_{in}(\mathbf{r}) = -\bar{\sigma}(\mathbf{r})\mathbf{B} \tag{1}$$

The three principal components are designated as follows

$$\sigma_{33} \geq \sigma_{22} \geq \sigma_{11} \tag{2}$$

The isotropic shielding $\sigma_{iso}(\mathbf{r})$ is one-third of the trace of $\bar{\sigma}(\mathbf{r})$.

In an NMR experiment, the isotropic chemical shift $\delta_{iso}(\mathbf{r})$ is measured, which is related to the isotropic shielding by

$$\delta_{iso}(\mathbf{r}) = -[\sigma_{iso}(\mathbf{r}) - \sigma_{ref}] \tag{3}$$

where σ_{ref} is the isotropic shielding of the nucleus in a reference system. For ^{17}O and ^{13}C, the references are liquid water and tetramethylsilane, respectively.

Rather than calculate the chemical shielding of the reference compound explicitly, we obtain σ_{ref} as the intercept of the graph of calculated shielding against experimental shift for D-glutamic acid·HCl. A least-squares fit gives $\sigma_{ref} = 255.0$ ppm for ^{17}O in reasonable agreement with previous studies.[11] For ^{13}C, a similar procedure gave a value of 170.1 ppm.

EFG. EFGs on the oxygen nuclei were calculated using the method of ref 11 with the PARATEC code and with the same input parameters as the chemical shielding calculations. The quadrupolar coupling constant, C_Q, and the asymmetry parameter, η, values were extracted from the diagonalized EFG tensor whose eigenvalues are labeled V_{xx}, V_{yy}, and V_{zz}, such that $|V_{zz}| > |V_{yy}| > |V_{xx}|$

$$C_Q = eV_{zz}Q_0/h \tag{4}$$

where h is Planck's constant and

$$\eta_Q = (V_{xx} - V_{yy})/V_{zz} \tag{5}$$

We use the experimental value of the electric quadrupole moment of the oxygen nucleus $Q_O = 2.55$ fm^2.[24]

3. Geometry

The relaxed crystal structures with the hydrogen bond distances labeled are shown in Figures 2−5 (crystal structures are available as Supporting Information). The improved accuracy of proton positions obtained from neutron diffraction over those from X-ray diffraction can be seen by considering the experimental and calculated O−H bond lengths, Table 1. The experimental hydroxyl bond length in DL-Glu, as found by X-ray diffraction, is rather short. Relaxing the DFT forces on the hydrogen atom gives an increase in the bond length of 0.06 Å.

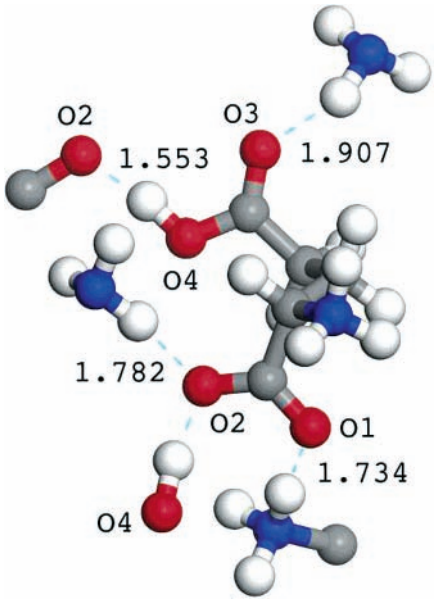

Figure 2. Hydrogen-bonding network in anhydrous α-L-glutamic acid. Oxygen sites are labeled, and hydrogen bond lengths are marked in angstroms.

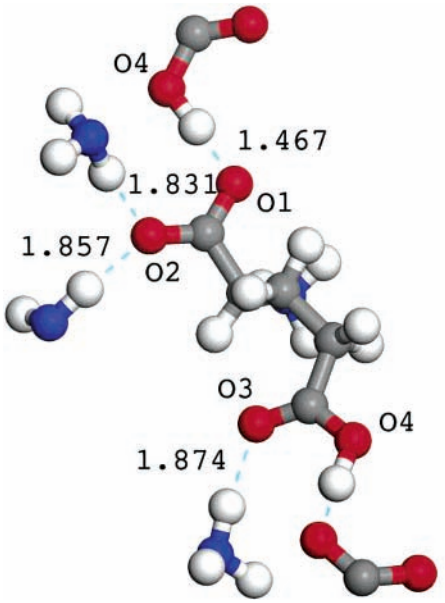

Figure 3. Hydrogen-bonding network in anhydrous β-L-glutamic acid. Oxygen sites are labeled, and hydrogen bond lengths are marked in angstroms.

For three of the four hydroxyl bond lengths from structures determined by neutron diffraction, relaxation of the forces leads to a small increase in the hydroxyl bond length of about 0.01 Å. The exception to this is the O4 hydroxyl bond in L-Glu·HCl, which increases in length by 0.04 Å.

4. L-Glutamic Acid·HCl

As an initial check of the validity of our approach, we first calculate the ^{13}C chemical shifts for L-Glu·HCl. As there are only five distinct carbon atoms in the crystal structure, the experimental ^{13}C spectrum is easy to assign. Figure 6 compares calculated and experimental ^{13}C chemical shifts for L-Glu·HCl. The agreement is very good, providing support for our calculation of ^{17}O shielding parameters.

The experimental ^{17}O shifts, quadrupolar coupling constants, and asymmetry parameters for L-Glu·HCl are summarized in

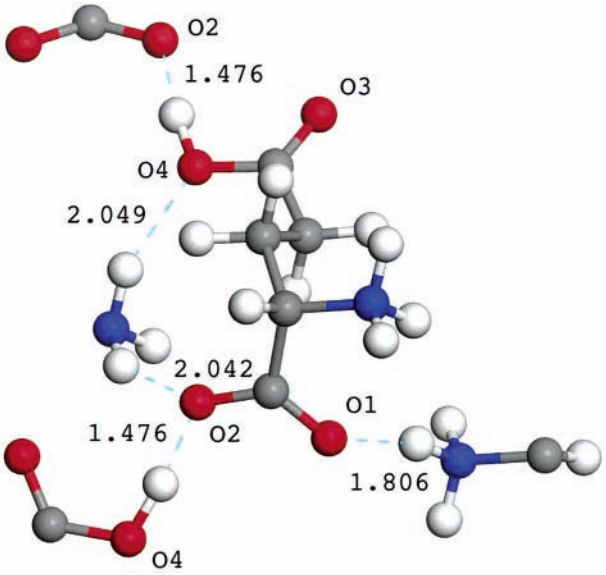

Figure 4. Hydrogen-bonding network in anhydrous DL-glutamic acid. Oxygen sites are labeled, and hydrogen bond lengths are marked in angstroms.

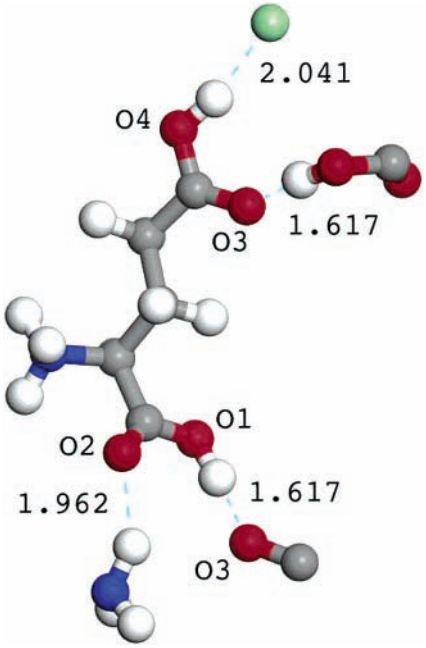

Figure 5. Hydrogen-bonding network in L-glutamic acid·HCl. Oxygen sites are labeled, and hydrogen bond lengths are marked in angstroms.

TABLE 1: Summery of Experimental and DFT-Optimized Hydroxyl Bond Lengths

structure	method	exp	relaxed
α L-glutamic acid	neutron	1.024[13]	1.037
β L-glutamic acid	neutron	1.049[14]	1.057
DL-glutamic acid	X-ray	0.991[15]	1.053
L-glutamic acid·HCl	neutron	1.016[16]	1.022
L-glutamic acid·HCl	neutron	0.981[16]	1.019

Table 2 together with the calculated parameters. In ref 6, the two peaks around 300 ppm in the spectra of L-Glu·HCl are attributed to the carbonyl oxygens and the peaks around 190 ppm to the hydroxyl oxygens. However, within each pair of peaks, no strong evidence was available to assign individual peaks to an atomic site.

Figure 7 shows a graph of the calculated ^{17}O shift plotted against experimental shift. The experimental separation between

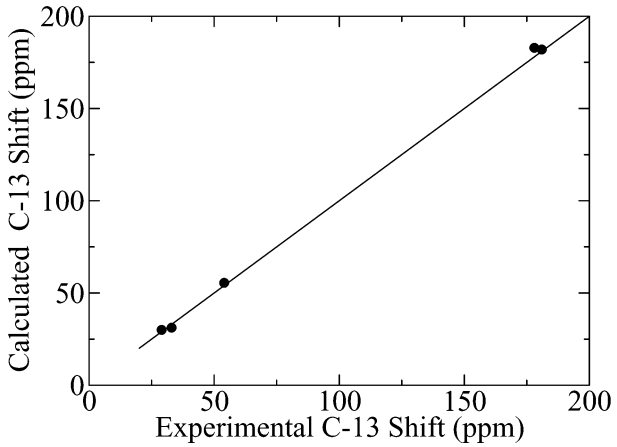

Figure 6. A graph of calculated vs experimental ^{13}C isotropic shift for L-glutamic acid·HCl. The line has unit gradients and represents perfect agreement between calculation and experiment.

TABLE 2: Calculated and Experimental ^{17}O NMR Parameters for L-Glutamic Acid·HCl[a]

calculated results				experimental results[6]			
atom	δ_{iso}(ppm)	C_Q(MHz)	η_Q	site	δ_{iso}(ppm)	C_Q(MHz)	η_Q
O1	177.6	7.72	0.22	4	172.5	7.45	0.25
O2	316.9	−8.61	0.12	1	322	8.16	0.0
O3	311.0	−8.90	0.23	2	315	8.31	0.17
O4	198.0	8.13	0.21	3	187	7.49	0.25

[a] Experimental data are taken from ref 6, assignment from section 4. Note that the experiment gives only the magnitude of C_Q.

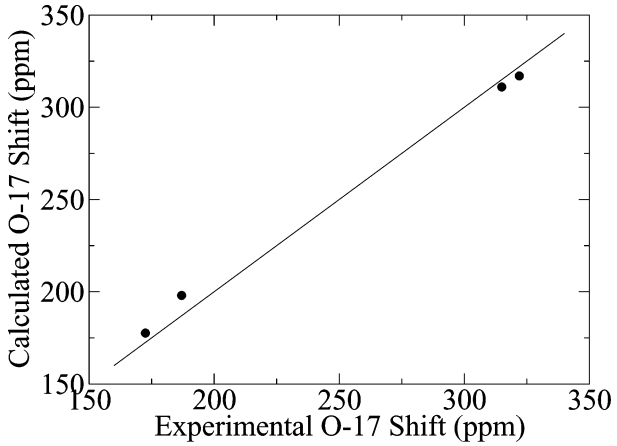

Figure 7. A graph of calculated vs experimental ^{17}O isotropic shift for L-glutamic acid·HCl. The line has unit gradients and represents perfect agreement between calculation and experiment.

the isotropic shift of the two carbonyl oxygens is 7.0 ± 1 ppm, which compares well with our calculated value of 5.9 ppm. The calculated separation of the hydroxyl oxygen peaks is 20.4 ppm in comparison to the measured value of 14.5 ± 1 ppm. On the basis of the calculated isotropic shifts, we assign the resonance at 172.5 ppm to O1, 187 ppm to O4, 315 ppm to O3, and 322 ppm to O2. Comparison of the experimental and calculated C_Q values, Table 2, also supports this assignment. The relative ordering of the sites is in agreement with the assignment based on the isotropic shift alone; however, the absolute calculated values are approximately 6% greater than in experiment. A similar systematic error has been noted in earlier quantum chemical studies of ^{17}O EFG for biological systems, which took account of this by using a scaled value of the oxygen electric quadrupole moment.[3] Three of the oxygen sites have very similar values of the asymmetry parameter, η_Q, and so we cannot draw definite conclusions from the calculated values of η_Q. The

TABLE 3: Calculated ^{17}O NMR Parameters for Anhydrous α-L-Glutamic Acid

atom	δ_{iso}(ppm)	C_Q(MHz)	η_Q
O1	289.1	−7.78	0.36
O2	280.0	−6.86	0.77
O3	320.4	−8.57	0.12
O4	201.2	7.61	0.10

TABLE 4: Calculated ^{17}O NMR Parameters for Anhydrous *β*-L-Glutamic Acid

atom	δ_{iso}(ppm)	C_Q(MHz)	η_Q
O1	264.2	−6.89	0.69
O2	291.5	−8.20	0.45
O3	323.2	−8.61	0.12
O4	205.7	7.58	0.27

TABLE 5: Calculated ^{17}O NMR Parameters for DL-Glutamic Acid

atom	δ_{iso}(ppm)	C_Q(MHz)	η_Q
O1	302.9	−8.55	0.30
O2	257.1	−7.24	0.72
O3	335.8	−9.18	0.01
O4	196.8	7.33	0.23

largest difference between experimental and calculated value of η_Q occurs for O4. Reference 6 gives an experimental value of 0.0. However it is worth noting that small values of η_Q are difficult to determine accurately, and so the experimental error on this point is rather large (∼0.05).

Further evidence in support of this assignment is given by the proton decoupling double rotation (DOR) experiments on glutamic acid·HCl by Pike et al.[25] In a DOR experiment with no proton decoupling, only the carbonyl oxygens are visible as the strong dipolar field from a proton at ∼1.0 Å broadens the lines from the hydroxyl oxygens beyond detection. The line widths of the two carbonyl oxygens with no decoupling are 280 ± 20 and 370 ± 30 Hz. At the low outer rotor spinning speeds used in a DOR experiment, one contribution to the residual line width is the proton dipolar field. This implies that the line with the larger line width corresponds to the site with the closer proton, i.e., O3 where the closest H is at 1.62 Å. This assignment was confirmed by applying a weak proton decoupling field of ∼28 kHz while the outer rotor was spinning at 1.8 kHz. The 280-Hz line narrowed, whereas the 370-Hz line broadened to ∼600 Hz. Investigations on L-alanine have shown that the broadening is due to a "rotary resonance" between the inner rotor spinning speed and the rf decoupling field,[25,26] which reintroduces the proton dipolar coupling. While the detailed theory of rotary resonance under DOR has not been worked out, it is clear that the oxygen DOR lines are affected very differently by the proton decoupling. The distance to the nearest hydrogen is very different for O2 and O3 (1.962 and 1.617 Å, respectively), which leads to the conclusion that the broader line most affected by proton decoupling is O3. This DOR line corresponds to site 2 in Table 2, i.e., the line with an isotropic shift of 315 ppm and the larger C_Q and asymmetry parameter in agreement with calculation.

5. Glutamic Acid Polymorphs

The calculated ^{17}O chemical shielding and electric field parameters for α-L-Glu, *β*-L-Glu, and DL-Glu are reported in Tables 3, 4, and 5, respectively. From Tables 2−5, it can be seen that all of the carbonyl oxygen shifts lie within the range 250−330 ppm and that the O−H oxygens are relatively more shielded and lie within the range 170−210 ppm. The ranges for the electric field parameters of carbonyl and OH oxygen overlap. To examine the effects of hydrogen bonding on these parameters we consider the carbonyl and hydroxyl sites separately.

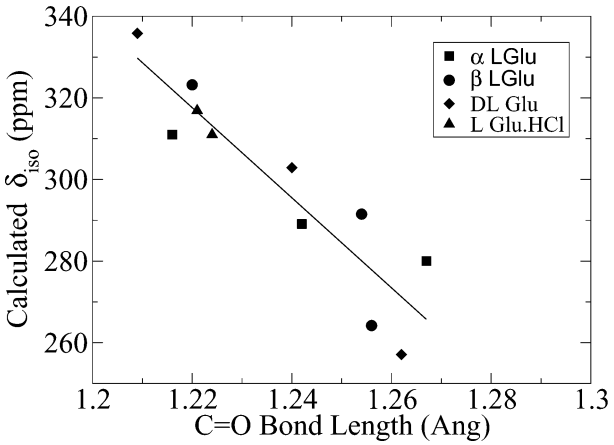

Figure 8. A graph of calculated ^{17}O isotropic chemical shift vs C═O bond length for glutamic acid polymorphs. The line represents the best linear fit.

Carbonyl Oxygens. Close examination of the crystal structures shows that the most deshielded carbonyl oxygen nucleus (O3 in DL-Glu at 335 ppm) has a very weak hydrogen bonded environment (O···H = 2.357 Å). The most shielded carbonyl oxygen nucleus (O2 in DL-Glu at 257.1 ppm) has a strong hydrogen bond (O···H = 1.476Å). It is therefore tempting to look for a correlation between the degree of hydrogen bonding and the ^{17}O chemical shifts.

Quantifying the strength of a hydrogen bond is a rather difficult task. For the structures studied, hydrogen bonds to both O−H and N−H groups are present with a mixture of 2- and 3-center hydrogen bonds. The only consistent parameter is the length of the carbonyl bond itself. A strong hydrogen-bonding environment will tend to increase the length of the carbonyl bond. For α amino acids, the side-chain moiety will have a much smaller effect than the hydrogen bond on the carbonyl bond length. It is then reasonable to look for a correlation between carbonyl bond length and a property which might depend on hydrogen bond strength.

Figure 8 shows a plot of calculated shielding against the C═O bond length. This confirms the general trend whereby increased hydrogen bond strength results in increased shielding of the carbonyl oxygen. The value of the linear regression coefficient, $r = -0.91$. While this is a reasonably good fit, it should be noted that even for these polymorphic systems such an empirical fit would not be accurate enough to reliably assign resonances.

Similar trends can be found for the quadrupolar coupling constants. Figure 9 is a plot of calculated value of C_Q against carbonyl bond length, and Figure 10 is the equivalent graph for η_Q. The regression coefficients are $r = -0.88$ and 0.97, respectively. Figure 9 shows that C_Q decreases with increasing hydrogen bond strength in agreement with earlier observations for similar systems.[3,5] Conversely, the asymmetry parameter increases with increasing hydrogen bond strength.

OH Oxygens. It is more difficult to draw definite conclusions about the effects of hydrogen bonding on the hydroxyl oxygens as there are only five such sites in the structures under consideration. Four sites have hydrogen bonds to carbonyl sites, while the fifth is hydrogen bonded to a chlorine ion.

Of the four hydroxyl oxygens hydrogen bonded to a carbonyl group, the most strongly shielded nucleus (O1 in L-Glu·HCl at 177.6 ppm) corresponds to a relatively weak hydrogen-bonded

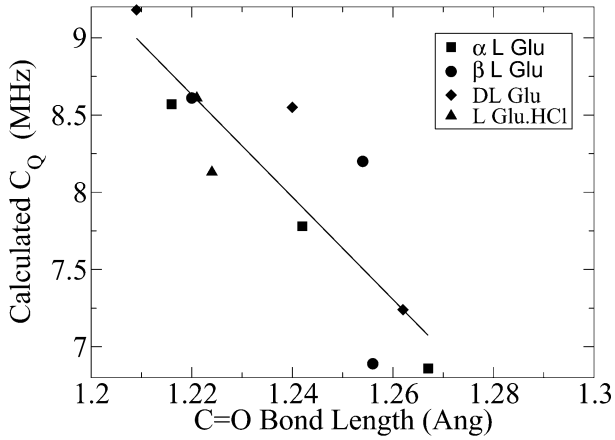

Figure 9. A graph of calculated ^{17}O C_Q magnitude vs C═O bond length. The line represents the best linear fit.

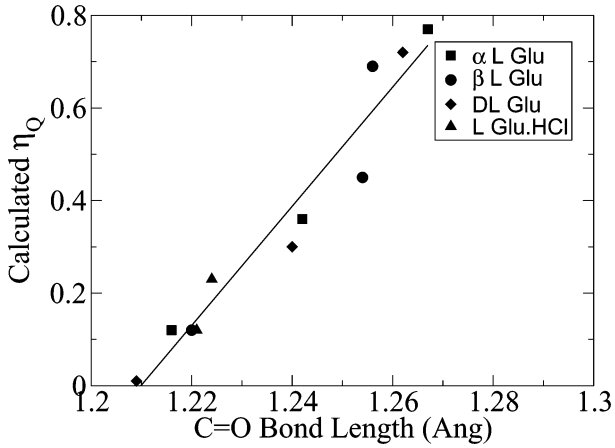

Figure 10. A graph of calculated ^{17}O electric field tensor asymmetry parameter, η_Q, vs C═O bond length. The line represents the best linear fit.

environment while the least shielded (O4 in β-L-Glu at 205.7 ppm) has a much stronger hydrogen bond.

The trend would seem to be the reverse of that for carbonyl oxygens, specifically because strong hydrogen-bonded environment deshields the oxygen nucleus. The range of chemical shifts (36 ppm) is much less than for carbonyl oxygens (80 ppm), showing a reduced sensitivity to hydrogen bonding.

The electric field parameters also show this reduced sensitivity to hydrogen bonding. C_Q varies from 7.33 to 8.13 MHz and η_Q between 0.10 and 0.27. There are no discernible trends in these values.

Other Reported NMR Spectra of Glutamic Acid. A rather different ^{17}O NMR spectrum of glutamic acid from that of Lemaitre et al.[6] has been presented by Wu and Dong.[3] This spectrum was analyzed as having a line at 170 ppm, $C_Q = 7.2$ MHz, $\eta_Q = 0.20$ (assigned to the hydroxyl site O4), another at 320 ppm with $C_Q = 8.2$ MHz, and $\eta_Q = 0$ (assigned to the hydroxyl site O1) with the two carbonyl sites having very similar shifts ~250 ppm, $C_Q = 6.8$ MHz and $\eta_Q = 0.58$. Although the two outer lines are in similar positions to those found by Lemaitre et al. for the hydroxyl and carbonyl sites, the inner peaks at 250 ppm were not observed and are well removed from the values calculated here. We note that on the basis of the calculations presented in this paper the peak observed by Wu and Dong at 320 ppm is most likely to be from a carbonyl oxygen. Lemaitre et al. suggested[6] that since the sample of Wu was enriched from an anhydrous DL-glutamic acid sample it may have been DL glutamic acid·HCl. Unfortunately there is no crystal structure in the literature for this compound. The shifts measured by Wu and Dong do not agree with any of the polymorphs calculated here, but it is interesting that anhydrous DL-glutamic acid does have one site, O2, with similar parameters, 256 ppm, $C_Q = 7.24$ MHz (which, when reduced by the 6% overestimate of the EFG, is 6.8 MHz), and $\eta_Q = 0.72$, to the intermediate line observed by Wu, which suggests that his sample might be a mixture of the different forms.

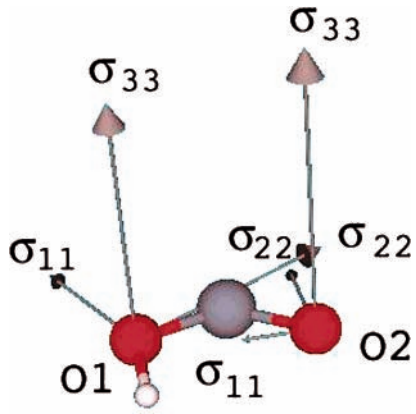

Figure 11. Directions and magnitudes of the principal axis of the chemical shielding tensor. α-carboxyl group in L-glutamic acid·HCl.

6. Principal Axis

Analysis of solid-state ^{17}O NMR spectra can yield the relative orientation between the EFG and chemical shielding tensors. However, technically difficult single-crystal experiments would be required to obtain the absolute tensor orientation relative to the molecular framework.

First-principles calculations automatically give the full tensor information, and the magnitudes and directions of the calculated principal components of the EFG and chemical shielding tensors of all the glutamic acid structures studied in this work are given in Tables S1−S4 of Supporting Information. Examination of the tensor components shows that while the magnitude of the principle components varies the orientation of the principal axis is similar for all carbonyl oxygens and for all hydroxyl oxygens. We focus on L-Glu·HCl and again discuss carbonyl and hydroxyl oxygens separately.

6.1. Carbonyl Oxygens. The most shielded component σ_{33} lies perpendicular to the plane of the carbonyl group, shown in Figures 11 and 12. The two largest components of the EFG tensor, V_{zz} and V_{yy}, lie within the plane of the carbonyl group. V_{zz} is perpendicular to the carbonyl bond, and V_{yy} lies along the carbonyl bond direction. V_{xx} is perpendicular to the plane of the carbonyl bond and is much smaller in magnitude than the other two components, shown in Figures 13 and 14.

6.2. Hydroxyl Oxygens. The two most shielded components of the chemical shielding tensor for the hydroxyl oxygen are almost equal in magnitude. The most shielded component, σ_{33}, is approximately perpendicular to the carbonyl plane, while σ_{22} lies roughly along the carbon−oxygen bond, as seen in Figures 11 and 12. The largest EFG component is roughly aligned with σ_{22}, as seen in Figures 13 and 14.

7. Conclusions

We have presented a theoretical investigation of ^{17}O chemical shielding and EFG parameters for polymorphs of glutamic acid. For L-glutamic acid·HCl, the agreement between experimental and calculated peaks is good and we can confidently assign the

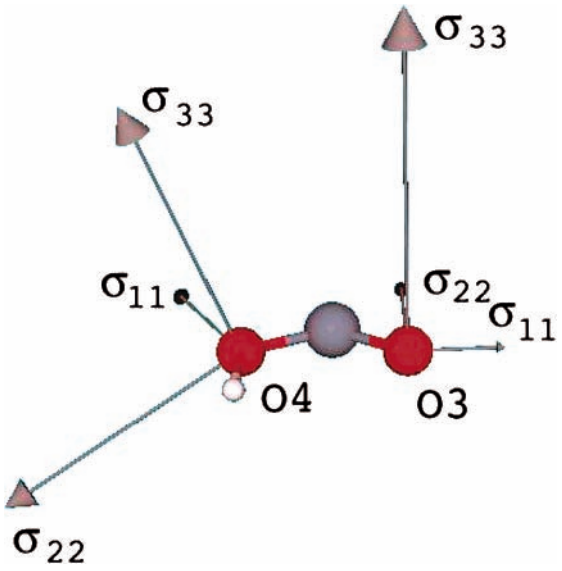

Figure 12. Directions and magnitudes of the principal axis of the chemical shielding tensor. γ-carboxyl group in L-glutamic acid·HCl.

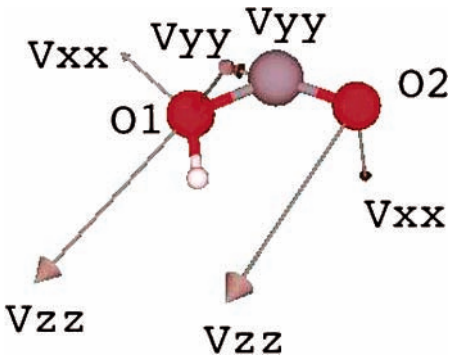

Figure 13. Directions and magnitudes of the principal axis of the EFG tensor. α-carboxyl group in L-glutamic acid·HCl.

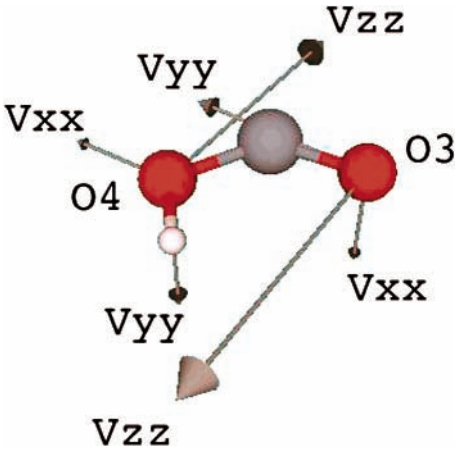

Figure 14. Directions and magnitudes of the principal axis of the EFG tensor. γ-carboxyl group in L-glutamic acid·HCl.

spectra. Our assignment is further supported by proton-decoupling DOR experiments.[25]

We believe that this type of first-principles calculation provides an important tool to complement solid-state NMR spectroscopy, not only to help assign difficult spectra but also to probe areas where experiments are difficult or time consuming. As an example, the extremely low natural abundance of ^{17}O meant that the sample of L-glutamic acid·HCl studied in ref 6 had to be enriched. This is a time-consuming and expensive process. By comparison, the first principles calculation of the EFG and NMR shielding tensors took approximately 4 h real time on an eight-processor IBM SP computer with Power4 processors.

By use of first-principles calculations, we are able to build on the original experimental result and efficiently study a range of glutamic acid polymorphs. Each polymorph has a different hydrogen bonding environment, which enables us to find correlations between ^{17}O NMR parameters and the strength of hydrogen bonding.

Acknowledgment. We wish to acknowledge the use of the EPSRC's Chemical Database Service at Daresbury. Computational resources were provided by the Cambridge-Cranfield High Performance Computing Facility. We acknowledge the support of Corpus Christi College, Cambridge (J.R.Y.), the UK Engineering and Physical Sciences Research Council (C.J.P., R.D.)

Supporting Information Available: DFT optimized crystal structures for the four glutamic acid structures (PDB). Tables S1−S4 give the full shielding and EFG tensors (PDF). This material is available free of charge via the Internet at http://pubs.acs.org.

References and Notes

(1) Kintzinger, J. P. Oxygen NMR Characteristic Parameters and Applications. In *NMR Basic Principles and Progress*; Diehl, P., Fluck, E., R. K., Eds.; Springer: New York, 1981.
(2) Klemperer, W. *Angew. Chem., Int. Ed. Engl.* **1978**, *17*, 246−254.
(3) Wu, G.; Dong, S. *J. Am. Chem. Soc.* **2001**, *123*, 9119−9125.
(4) Wu, G.; Dong, S.; Ida, R.; Reen, N. *J. Am. Chem. Soc.* **2001**, *124*, 1768.
(5) Howes, A.; Jenkins, R.; Smith, M.; Crout, D.; Dupree, R. *Chem. Commun.* **2001**, *16*, 1448−1449.
(6) Lemaitre, V.; Pike, K.; Watts, A.; Anupold, T.; Samoson, A.; Smith, M.; Dupree, R. *Chem. Phys. Lett.* **2003**, *371*, 91−97.
(7) *Calculation of NMR and EPR Parameters. Theory and Applications*; Kaupp, M., Bühl, M., Malkin, V., Eds.; Wiley VCH: Weinheim, 2004.
(8) Helgaker, T.; Jaszunski, M.; Ruud, K. *Chem. Rev.* **1999**, *99*, 293−353.
(9) Pickard, C.; Mauri, F. *Phys. Rev B* **2001**, *63*, 245101.
(10) Payne, M.; Teter, M.; Allen, D.; Arias, T.; Joannopoulos, J. *Rev. Mod. Phys.* **1992**, *64*, 1045−1097.
(11) Profeta, M.; Mauri, F.; Pickard, C. J. *J. Am. Chem. Soc.* **2003**, *125*, 541−548.
(12) Bull, L.; Bussemer, B.; Anupold, T.; Reinhold, A.; Samoson, A.; Sauer, J.; Cheetham, A.; Dupree, R. *J. Am. Chem. Soc.* **2000**, *122*, 4948−4958.
(13) Lehmmann, M.; Nunes, A. *Acta Cryst* **1980**, *B36*, 1621−1625.
(14) Lehmmann, M.; Koetzle, T. F.; Hamilton, W. *J. Cryst. Mol. Struct.* **1972**, *2*, 225−233.
(15) Dunitz, J.; Schweizer, W. *Acta Crystallogr.* **1995**, *C51*, 1337−1379.
(16) Sequeira, A.; Rajagopal, H.; Chidambaram, R. *Acta Crystallogr.* **1972**, *B*, 2514.
(17) Fletcher, D.; McMeeking, R.; Parkin, D. *J. Chem. Inf. Comput. Sci.* **1996**, *36*, 746−749.
(18) Jeffrey, G. *An Introduction to Hydrogen Bonding*; Oxford University Press: Oxford, UK, 1997.
(19) Segall, M.; Lindan, P.; Probert, M.; Pickard, C.; Hasnip, P.; Clark, S.; Payne, M. *J. Phys.: Condens. Matter* **2002**, *14*, 2717−2743.
(20) Perdew, J. P.; Burke, K.; Ernzerhof, M. *Phys. Rev. Lett.* **1996**, *77*, 3865−3868.
(21) Vanderbilt, D. *Phys. Rev. B* **1990**, *41*, 7892−7895.
(22) Calculations were performed with PARATEC (PARAllel Total Energy Code) by: Pfrommer, B.; Raczkowski, D.; Canning, A.; Louie, S. G. (with contributions from Mauri, F.; Cote, M.; Yoon, Y.; Pickard, C.; Haynes, P.). Lawrence Berkeley National Laboratory. For more information, see: www.nersc.gov/projects/paratec.
(23) Troullier, N.; Martins, J. *Phys. Rev. B* **1991**, *43*, 1993−2006.
(24) Pyykkö, P. *Mol. Phys.* **2001**, *99*, 1617−1629.
(25) Pike, K.; Lemaitre, V.; Kukol, A.; Anupold, T.; Samosen, A.; Howes, A.; Watts, A.; Smith, M.; Dupree, R. *J. Phys. Chem. B*, in press.
(26) Wi, S.; Logan, J.; Sakellariou, D.; Walls, J.; Pines, A. *J. Chem. Phys.* **2002**, *117*, 7024.